Eur. Phys. J. C 52, 187–201 (2007)
DOI 10.1140/epjc/s10052-007-0368-6

THE EUROPEAN PHYSICAL JOURNAL C

Regular Article – Theoretical Physics

Thermal hadronization and Hawking–Unruh radiation in QCD

P. Castorina[1], D. Kharzeev[2,a], H. Satz[3]

[1] Dipartimento di Fisica, Università di Catania, and INFN Sezione di Catania, Via Santa Sofia 64, 95123 Catania, Italy
[2] Physics Department, Brookhaven National Laboratory, Upton, NY 11973-5000, USA
[3] Fakultät für Physik, Universität Bielefeld, 33501 Bielefeld, Germany

Received: 13 April 2007 / Revised version: 16 June 2007 /
Published online: 27 July 2007 –

Abstract. We conjecture that, because of color confinement, the physical vacuum forms an event horizon for quarks and gluons, which can be crossed only by quantum tunneling, i.e., through the QCD counterpart of Hawking radiation at black holes. Since such radiation cannot transmit information to the outside, it must be thermal, of a temperature determined by the chromodynamic force at the confinement surface, and it must maintain color neutrality. We explore the possibility that the resulting process provides a common mechanism for thermal hadron production in high energy interactions, from e^+e^- annihilation to heavy ion collisions.

PACS. 04.70.Dy; 12.38.Aw; 12.38.Mh; 12.40.Ee; 25.75.Nq; 97.60.Lf

1 Introduction

The aim of this paper is to develop a conceptual framework for a universal form of thermal multihadron production in high energy collisions. Our work is based on two seemingly disjoint observations.

- Color confinement in QCD does not allow colored constituents to exist in the physical vacuum, and thus in some sense creates a situation similar to the gravitational confinement provided by black holes.
- Numerous high energy collision experiments have provided strong evidence for the thermal nature of multihadron production, indicating a universal hadronization temperature $T_{\rm H} \simeq 150$–$200\,{\rm MeV}$.

We want to suggest that quantum tunneling through a color event horizon, as a QCD counterpart of Hawking–Unruh radiation from black holes, can relate these observations in a quite natural way.

The idea that the color confinement of quarks and gluons in hadrons may have a dual description in terms of a theory in curved space-time is not new. Both gravitational confinement of matter inside a black hole [1] and the de Sitter solution of the Einstein equations with a cosmological constant describing a "closed" universe of constant curvature [2, 3] have been proposed as possible descriptions of quark confinement. Soon it became clear that asymptotic freedom [4, 5] and the scale anomaly [6–11] in QCD completely determine the structure of low-energy gluodynamics [12]. This effective theory can be conveniently formulated in terms of the Einstein–Hilbert action in a curved background. At shorter distances (inside hadrons), the effective action has the form of classical Yang–Mills theory in a curved (but conformally flat) metric [13, 14]. The "cosmological constant" present in this theory corresponds to the non-perturbative energy density of the vacuum, or the "gluon condensate" [15].

It is worthwhile to also mention here the well-known conjectured holographic correspondence between the large N limit of supersymmetric Yang–Mills theory in $3+1$ dimensions and supergravity in an anti-de Sitter space-time sphere, $AdS_5 \times S_5$ [16]. This example illustrates the possible deep relation between Yang–Mills theories and gravity; however, a conformal theory clearly differs from the examples noted above, in which the scale anomaly (describing the breaking of conformal invariance by quantum effects) was used as a guiding principle for constructing an effective curved space-time description.

Let us assume that color confinement indeed allows for a dual description in terms of the gravitational confinement of matter inside black holes. What are the implications of this hypothesis for hadronic physics? Hawking [17] showed that black holes emit thermal radiation due to quantum tunneling through the event horizon. Shortly afterwards, Unruh [18] demonstrated that the presence of an event horizon in accelerating frames also leads to thermal radiation. It was soon conjectured that the periodic motion of quarks in a confining potential [19], or the acceleration which accompanies inelastic hadronic collisions [20–22], are associated with an effective temperature for hadron emission.

Recently, a QCD-based picture of thermal production based on the parton description of high energy hadronic collisions has been proposed [23–25]. The effective tem-

[a] e-mail: kharzeev@bnl.gov

perature T is in this case determined either by the string tension σ, with the relation

$$T = \sqrt{\frac{3\sigma}{4\pi}}\,, \tag{1}$$

or, in the gluon saturation regime, by the saturation momentum $Q_{\rm s}$ describing the strength of the color fields in the colliding hadrons or nuclei, with $T \simeq (Q_{\rm s}/2\pi)$.

Turning now to the second observation, we recall that over the years, hadron production studies in a variety of high energy collision experiments have shown a remarkably universal feature. From e^+e^- annihilation to p–p and p–$\bar{p}$ interactions and further to collisions of heavy nuclei, with energies from a few GeV up to the TeV range, the production pattern always shows striking thermal aspects, connected to an apparently quite universal temperature around $T_{\rm H} \simeq 150$–$200\,\mathrm{MeV}$ [26, 27]. As a specific illustration we recall that the relative abundance of two hadron species a and b, of masses m_a and m_b, respectively, is essentially determined by the ratio of their Boltzmann factors [28–32],

$$R(a/b) \sim \exp -\{(m_a - m_b)/T_{\rm H}\}\,. \tag{2}$$

What is the origin of this thermal behavior? While high energy heavy ion collisions involve large numbers of incident partons and thus could allow for invoking some "thermalization" scheme through rescattering, in e^+e^- annihilation the predominant initial state is one energetic $q\bar{q}$ pair, and the number of hadronic secondaries per unit rapidity is too small to consider statistical averages. The case in p–p/p–$\bar{p}$ collisions is similar.

This enigma has led to the idea that all such collision experiments result in the formation of a strong color field "disturbing" the physical vacuum. The disturbed vacuum then recovers by producing hadrons according to a maximum entropy principle: the actually observed final state is that with the largest phase space volume. While this provides an intuitive basis for a statistical description, it does not account for a universal temperature. Why do not more energetic collisions result in a higher hadronization temperature?

A further piece in this puzzle is the observation that the value of the temperature determined in the mentioned collision studies is quite similar to the confinement/deconfinement transition temperature found in lattice studies of strong interaction thermodynamics[1]. While hadronization in high energy collisions deals with a dynamical situation, the energy loss of fast color charges "traversing" the physical vacuum, lattice QCD addresses the equilibrium thermodynamics of unbound versus bound color charges. Why should the resulting critical temperatures be similar or even identical?

We shall here consider these phenomena as reflections of the QCD counterpart of the Hawking radiation emitted by black holes [17]. These ultimate stellar states provide a gravitational form of confinement and hence, as already noted, their physics was quite soon compared to that of color confinement in QCD [1–3], where colored constituents are confined to "white holes" (colorless from the outside, but colored inside). It should be emphasized from the outset that in contrast to the original black hole physics in gravitation, where confinement is on a classical level complete, in QCD confinement refers only to color-carrying constituents; thus, e.g., photons or leptons are not affected.

In black hole physics, as noted above, it was shown that the event horizon for systems undergoing uniform acceleration leads to quantum tunneling and hence to thermal radiation [18]. Our aim here is to show that such Hawking–Unruh radiation, as obtained in the specific situation of QCD, provides a viable account for the thermal behavior observed in multihadron production by high energy collisions. Furthermore, in the process we also want to elucidate a bit the common origin of the "limiting temperature" concepts that have arisen in strong interaction physics over the years.

We begin by reviewing those features of black hole physics and Hawking radiation that are relevant for our considerations and then discuss how they can be implemented in QCD. In particular, we show that modifications of the effective space-time structure, in a perturbative approach as well as in a non-perturbative treatment based on a large-scale dilaton field, lead to an event horizon in QCD.

Following this, we present the main conceptual consequences of our conjecture.

- Color confinement and the instability of the physical vacuum under pair production form an event horizon for quarks, allowing for a transition only through quantum tunneling; this leads to thermal radiation of a temperature $T_{\rm Q}$ determined by the string tension.
- Hadron production in high energy collisions occurs through a succession of such tunneling processes. The resulting cascade is a realization of the same partition process as leads to a limiting temperature in the statistical bootstrap and dual resonance models.
- The temperature $T_{\rm Q}$ of QCD Hawking–Unruh radiation can depend only on the baryon number and the angular momentum of the deconfined system. The former could provide a dependence of $T_{\rm Q}$ on the baryon number density, while the angular momentum pattern of the radiation allows for a centrality dependence of $T_{\rm Q}$ and elliptic flow.
- In kinetic thermalization, the initial state information is successively lost through collisions, converging to a time-independent equilibrium state. In contrast, the stochastic QCD Hawking radiation is "born in equilibrium", since quantum tunneling a priori does not allow for information transfer.

2 Event horizons in gravitation and in QCD

2.1 Black holes

A black hole is formed as the final stage of a neutron star after gravitational collapse [37]. It has a mass M concentrated in such a small volume that the resulting gravita-

[1] See e.g., [33] for the latest state and references to earlier work.

tional field confines all matter and even photons to remain inside the event horizon R of the system: no causal connection with the outside is possible. As a consequence, black holes have three (and only three) observable properties: mass M, charge Q and angular momentum J. This section will address mainly black holes with $Q = J = 0$; we shall come back to the more general properties in Sect. 4. We use units of $\hbar = c = 1$.

The event horizon appears in a study of the gravitational metric, which in flat space has the form

$$\mathrm{d}s^2 = g\,\mathrm{d}t^2 - g^{-1}\,\mathrm{d}r^2 - r^2[\,\mathrm{d}\theta^2 + \sin^2\theta\,\mathrm{d}\phi^2]\,, \qquad (3)$$

using units where $c = 1$. The field strength of the interaction is contained in the coefficient $g(r)$,

$$g(r) = \left(1 - \frac{2GM}{r}\right)\,, \qquad (4)$$

leading back to the Minkowski metric in the large distance limit $r \to \infty$. The vanishing of $g(r)$ specifies the Schwarzschild radius R as the event horizon,

$$R = 2GM\,. \qquad (5)$$

It is interesting to note that the mass of a black hole thus grows linearly with R, analogous to the behavior of the confining potential in strong interactions: $M(R) = (2G)^{-1}R$.

Classically, a black hole would persist forever and remain forever invisible. On a quantum level, however, its constituents (photons, leptons and hadrons) have a non-vanishing chance to escape by tunneling through the barrier presented by the event horizon. Equivalently, we can say that the strong force field at the surface of the black hole can bring vacuum fluctuations on-shell. The resulting Hawking radiation [17] cannot convey any information about the internal state of the black hole; it must be therefore be thermal. For a non-rotating black hole of vanishing charge (denoted as Schwarzschild black hole), the first law of thermodynamics,

$$\mathrm{d}M = T\,\mathrm{d}S \qquad (6)$$

combined with the area law for the black hole entropy [38],

$$S = \frac{\pi R^2}{G} \qquad (7)$$

leads to the corresponding radiation temperature

$$T_{\mathrm{BH}} = \frac{1}{8\pi GM}\,. \qquad (8)$$

This temperature is inversely proportional to the mass of the black hole, and since the radiation reduces the mass, the radiation temperature will increase with time, as the black hole evaporates. For black holes of stellar size, however, one finds $T_{\mathrm{BH}} \lesssim 2 \times 10^{-8}\,\mathrm{K}$, which is many orders of magnitude below the 2.7 K cosmic microwave background, and it hence is not detectable.

It is instructive to consider the Schwarzschild radius of a typical hadron, assuming a mass $m \sim 1\,\mathrm{GeV}$:

$$R_g^{\mathrm{had}} \simeq 1.3 \times 10^{-38}\,\mathrm{GeV}^{-1} \simeq 2.7 \times 10^{-39}\,\mathrm{fm}\,. \qquad (9)$$

To become a gravitational black hole, the mass of the hadron would thus have to be compressed into a volume more than 10^{100} times smaller than its actual volume, with a radius of about 1 fm. On the other hand, if instead we increase the interaction strength from gravitation to strong interaction [1], we gain in the resulting "strong" Schwarzschild radius $R_{\mathrm{s}}^{\mathrm{had}}$ a factor

$$\frac{\alpha_{\mathrm{s}}}{Gm^2}\,, \qquad (10)$$

where α_{s} is the dimensionless strong coupling and Gm^2 the corresponding dimensionless gravitational coupling for the case in question. This leads to

$$R_{\mathrm{s}}^{\mathrm{had}} \simeq \frac{2\alpha_{\mathrm{s}}}{m}\,; \qquad (11)$$

with the effective value of $\alpha_{\mathrm{s}} \sim \mathcal{O}(1)$ we thus get $R_{\mathrm{s}}^{\mathrm{had}} \sim \mathcal{O}(1)$ fm.[2] In other words, the confinement radius of a hadron is about the size of its "strong" Schwarzschild radius, so that we could consider quark confinement as the strong interaction version of the gravitational confinement in black holes [1–3].

We have seen that the mass of a black hole grows linearly with the event horizon, $M = (1/2G)R$, so that in gravitation $1/2G$ plays the role of the string tension in strong interaction physics. The replacement $GM^2 \to \alpha_{\mathrm{s}}$ here leads to

$$\sigma \simeq \frac{m^2}{2\alpha_{\mathrm{s}}} \simeq 0.16\,\mathrm{GeV}^2\,, \qquad (12)$$

if one uses the mentioned effective saturation value $\alpha_{\mathrm{s}} \simeq 3$ [39]. The value of $\alpha_{\mathrm{s}} \sim 1$ thus gives a reasonable string tension as well as a reasonable radius.

2.2 Quasi-Abelian case

The appearance of an event horizon occurs in general relativity through the modification of the underlying space-time structure by the gravitational interaction. Such modifications have also been discussed for other interactions. In particular, it was noted that in electrodynamics, nonlinear in-medium effects can lead to photons propagating along geodesics that are not null in Minkowski space-time; this can even lead to photon trapping, restricting the motion of photons to a compact region of space [40]. Thus, an effective Lagrangian $\mathcal{L}(F)$ depending on a one-parameter background field, $F = F_{\mu\nu}F^{\mu\nu}$, results in a modified metric

$$g_{\mu\nu} = \eta_{\mu\nu}\mathcal{L}' - 4F_{\alpha\mu}F^{\alpha}_{\nu}\mathcal{L}''\,, \qquad (13)$$

[2] In fact, some studies [39] indicate that at large distances, the strong coupling freezes at $\alpha_{\mathrm{s}} \simeq 3$; in that case the corresponding radius becomes $R_{\mathrm{s}}^{\mathrm{had}} \simeq 1$ fm.

where the primes indicate first and second derivatives with respect to F. Hence

$$g_{00} = \mathcal{L}' - 4F\mathcal{L}'' = 0 \tag{14}$$

defines the radius of the compact region of the theory, i.e., the counterpart of a black hole [40].

QCD is an inherently non-linear theory, with the physical vacuum playing the role of a medium [41]. The general structure of the effective Lagrangian in a background field F, compatible with gauge invariance, renormalization group results [4, 5] and trace anomaly, has the unique form [42–45]

$$\mathcal{L}_{\rm QCD} = \frac{1}{4}F_{\mu\nu}F^{\mu\nu}\frac{g^2(0)}{g^2(gF)} = \frac{1}{4}F_{\mu\nu}F^{\mu\nu}\epsilon(gF)\,. \tag{15}$$

Here $\epsilon(gF)$ is the dielectric "constant" of the system in the presence of the background field; the F-dependence of $\epsilon(F)$ effectively turns the QCD vacuum into a non-linear medium. On a one-loop perturbative level we have

$$\epsilon(gF) \simeq 1 - \beta_0\left(\frac{g^2}{4\pi}\right)\ln\frac{\Lambda^2}{gF}\,, \tag{16}$$

where $\beta_0 = (11N_c - 2N_f)/48\pi^2$, with N_c and N_f specifying the number of colors and flavors, respectively. Using this form in the formalism of [40] leads to g_t changing sign (i.e., $g_t = 0$) at

$$gF^* = \Lambda^2\exp\left\{-4\pi/\beta_0 g^2\right\}\,, \tag{17}$$

indicating a possible horizon at $r^* \sim 1/\sqrt{gF^*}$ [46]. It is clear that this line of argument can at best provide some hints, since we used the lowest order perturbative form of the beta-function, even though at the horizon perturbation theory will presumably break down. Nevertheless, we believe that it suggests the possibility of an event horizon for QCD; the crucial feature is the asymptotic freedom of QCD [4, 5], which leads to $\epsilon < 1$ and allows g_{00} to vanish even without the external medium effects required in QED.

2.3 Non-Abelian case

Indeed, a different and more solid suggestion that in QCD there is an event horizon comes from studying the theory on a curved background. For gluodynamics, such a program is discussed in [13, 14]. Classical gluodynamics is a scale-invariant theory, but quantum fluctuations break this invariance, with the trace of the energy-momentum tensor introducing non-perturbative effects, associated with the vacuum energy density $\epsilon^{\rm vac}$. It was shown [12] that low-energy theorems can be used to determine the form of the effective Yang–Mills Lagrangian in a curved but conformally flat metric

$$g_{\mu\nu}(x) = \eta_{\mu\nu}e^{h(x)}\,, \tag{18}$$

where the dilaton field $h(x)$ is coupled to the trace of the energy-momentum tensor, θ^μ_μ. The resulting action has the form

$$S = \int {\rm d}^4x \times\left[\frac{4}{3}\frac{\epsilon^{\rm vac}}{m_G^2}e^h(\partial_\mu h)^2 - \frac{1}{4}(F^a_{\mu\nu})^2 + e^{2h}\left(\epsilon^{\rm vac} - \frac{1}{4}\theta^\mu_\mu|_{\rm pert}\right)\right]; \tag{19}$$

here $\epsilon^{\rm vac}$ is the absolute value of the energy density of the vacuum and m_G the dilaton mass; the trace of the energy-momentum tensor has been separated into perturbative and non-perturbative contributions,

$$\theta^\mu_\mu = \theta^\mu_\mu\big|_{\rm pert} + \langle\theta^\mu_\mu\rangle = \theta^\mu_\mu\big|_{\rm pert} - 4\epsilon^{\rm vac}\,. \tag{20}$$

The crucial point for our considerations is that the first term of (19) can be written as

$$\frac{3}{2}e^h\left(\partial_\mu h\right)^2 = R\sqrt{-g}\,, \tag{21}$$

defining R as the Ricci scalar of the theory. Hence (19) has the structure of an Einstein–Hilbert Lagrangian of gluodynamics in the presence of an effective gravitation,

$$S_G = \int {\rm d}^4x\left[\frac{\sqrt{-g}}{8\pi G}R - \frac{1}{4}\left(F^a_{\mu\nu}\right)^2 + e^{2h}\left(\epsilon^{\rm vac} - \frac{1}{4}\theta^\mu_\mu|_{\rm pert}\right)\right]; \tag{22}$$

where G is now given by

$$\frac{1}{G} = \frac{64\pi}{3}\frac{\epsilon^{\rm vac}}{m_G^2}\,. \tag{23}$$

The relation $1/2G \to \sigma$ between G and the string tension conjectured above then leads to

$$\sigma = \frac{32\pi}{3}\frac{\epsilon^{\rm vac}}{m_G^2}\,. \tag{24}$$

On the other hand, the string tension is just the energy density of the vacuum times the transverse string area,

$$\sigma = \epsilon^{\rm vac}\pi r_{\rm T}^2\,. \tag{25}$$

Combining relations (24) and (25), we have

$$r_{\rm T} = \sqrt{\frac{32}{3}}\frac{1}{m_G} \simeq 0.4\,{\rm fm}\,, \tag{26}$$

using $m_G \simeq 1.5\,{\rm GeV}$ for the scalar glueball mass. Equation (26) thus gives us the transverse extension or horizon of the string.

From (24) or (25) we can obtain a further consistency check. Given the glueball mass and the string tension $\sigma \simeq 0.16\,{\rm GeV}^2$, we find for the vacuum energy density

$$\epsilon^{\rm vac} \simeq \frac{3}{32\pi}\sigma m_G^2 \simeq 0.013\,{\rm GeV}^4 \simeq 1.7\,{\rm GeV/fm}^3\,. \tag{27}$$

This is the value for pure gluodynamics; since the energy density is related to the trace of the energy-momentum tensor by the relation (20), and

$$\theta^{\mu}_{\mu} = \frac{\beta(g)}{2g}\left(F^{a}_{\mu\nu}\right)^2 \simeq -b\frac{g^2}{32\pi^2}\left(F^{a}_{\mu\nu}\right)^2 , \qquad (28)$$

with the coefficient $b = 11N_c - 2N_f$ of the β-function, we can estimate that for three-flavor QCD

$$\epsilon^{\rm vac}_{\rm QCD} = \frac{11N_c - 2N_f}{11N_c}\epsilon^{\rm vac} = \frac{9}{11}\epsilon^{\rm vac} \simeq 0.01\ {\rm GeV}^4 , \qquad (29)$$

which is in perfect agreement with the original value of the gluon condensate [15]

$$\left\langle \frac{\alpha_{\rm s}}{\pi} G^2 \right\rangle \simeq 0.012\ {\rm GeV}^4 ; \qquad (30)$$

note that $\epsilon^{\rm vac}_{\rm QCD} = 27/32\,\langle(\alpha_{\rm s}/\pi)G^2\rangle$.

3 Hyperbolic motion and Hawking–Unruh radiation

In general relativity, the event horizon appeared as a consequence of the geometrized gravitational force, but its occurrence and its role for thermal radiation was soon generalized by Unruh [18]. A system undergoing uniform acceleration a relative to a stationary observer eventually reaches a classical turning point and thus encounters an event horizon. Let us recall the resulting hyperbolic motion[3]. A point mass m subject to a constant force F satisfies the equation of motion

$$\frac{\rm d}{{\rm d}t}\frac{mv}{\sqrt{1-v^2}} = F , \qquad (31)$$

where $v(t) = {\rm d}x/{\rm d}t$ is the velocity, normalized to the speed of light $c = 1$. This equation is solved by the parametric form through the so-called Rindler coordinates,

$$x = \xi\cosh a\tau \quad t = \xi\sinh a\tau , \qquad (32)$$

where $a = F/m$ denotes the acceleration in the instantaneous rest frame of m, and τ the proper time, with ${\rm d}\tau = \sqrt{1-v^2}\,{\rm d}t$. If we impose the boundary condition that the velocity at $t = 0$ vanishes, we have $\xi = 1/a$ and $x(t = 0) = 1/a$. The resulting world line is shown in Fig. 1. It corresponds to the mass m coming from $x = \infty$ at $t = -\infty$ with a velocity arbitrarily close to that of light, decelerating uniformly until it comes to rest at the classical turning point $x_{\rm H} = -(1/a), t = 0$. Subsequently, it accelerates again and returns to $x = \infty$ at $t = \infty$, approaching the speed of light. For given a, the light cone originating at a distance $x_{\rm H} = 1/a$ away from the turning point of m defines a space-time region inaccessible to m: no photon in this region can (classically) ever reach m, in much the same way as photons cannot escape from a black hole. Here the acceleration is crucial, of course; if m stops accelerating, it will eventually become visible in the "hidden region".

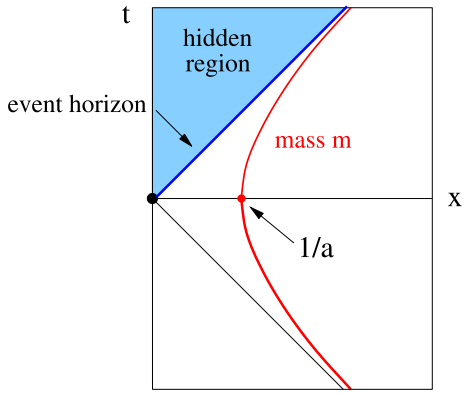

Fig. 1. Hyberbolic motion

The metric of such an accelerating system becomes in spherical coordinates [47]

$${\rm d}s^2 = \xi^2 a^2\,{\rm d}\tau^2 - {\rm d}\xi^2 - \xi^2\cosh^2 a\tau({\rm d}\theta^2 + \sin^2\theta\,{\rm d}\phi^2) , \qquad (33)$$

which we want to compare to the black hole metric (3). Making in the latter the coordinate transformation [48]

$$\eta = \frac{\sqrt{g}}{\kappa} , \qquad (34)$$

where the surface gravity κ is given by

$$\kappa = \frac{1}{2}\left(\frac{\partial g}{\partial r}\right)_{r=R} , \qquad (35)$$

we obtain for $r \to R$ the black hole form

$${\rm d}s^2 = \eta^2\kappa^2\,{\rm d}t^2 - {\rm d}\eta^2 - R^2({\rm d}\theta^2 + sin^2\theta\,{\rm d}\phi^2) . \qquad (36)$$

When we compare (33) and (36), it is evident that the system in uniform acceleration can be mapped onto a spherical black hole, and vice versa, provided we identify the surface gravity κ with the acceleration a.

The vacuum through which m travels is, for a stationary observer, empty space. On a quantum level, however, it contains vacuum fluctuations. The accelerating mass m can bring these on-shell, using up a (small) part of its energy, so that for m the vacuum becomes a thermal medium of temperature

$$T_{\rm U} = \frac{a}{2\pi} . \qquad (37)$$

Consider such a fluctuation into an e^+e^- pair, flying apart in opposite directions. One electron is absorbed by the mass m, the other penetrates into the "hidden region" and can never be detected by m (see Fig. 2). Since thus neither an observer on m nor a stationary observer in the hidden region can ever obtain access to full information, each will register the observed radiation as thermal (Einstein–Podolsky–Rosen effect [49, 50]). In other words: the accelerating mass m sees the vacuum as a physical medium of

[3] For a clear discussion and references to the original solutions by M. Born (1909) and A. Sommerfeld (1910), see [51].

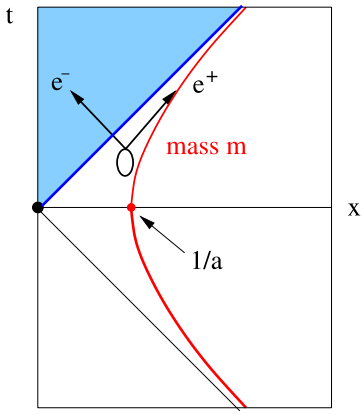

Fig. 2. Unruh radiation

temperature $T_{\rm U}$, while a stationary observer in the hidden region observes thermal radiation of temperature $T_{\rm U}$ as a consequence of the passing of m.

We here also mention that the entropy in the case of an accelerating system again becomes 1/4 of the event horizon area, as in the black hole case, so that also here the correspondence remains valid [52].

In the case of gravity, we have the force

$$F = ma = G\frac{mM}{R^2}\,, \tag{38}$$

on a probe of mass m. With $R = 2GM$ for the (Schwarzschild) black hole radius, we have $a = 1/(4GM)$ for the acceleration at the event horizon and hence the Unruh temperature (37) leads back to the Hawking temperature of (8).

In summary, we note that constant acceleration leads to an event horizon, which can be surpassed only by quantum tunneling and at the expense of complete information loss, leading to thermal radiation as the only resulting signal.

4 Pair production and string breaking

In the previous section, we have considered a classical object, the mass m, undergoing accelerated motion in the physical vacuum; because of quantum fluctuations, this vacuum appears to m as a thermal medium of temperature $T_{\rm U}$. In this section, we shall first address the modifications that arise if the object undergoing accelerated motion is itself a quantum system, so that in the presence of a strong field it becomes unstable under pair production. Next we turn to the specific additional features that come in when the basic constituents are subject to color confinement and can only exist in color neutral bound states.

As a starting point, we consider two-jet e^+e^- annihilation at CMS energy $\sqrt{s}$,

$$e^+e^- \to \gamma^* \to q\bar{q} \to \text{ hadrons}\,. \tag{39}$$

The initially produced $q\bar{q}$ pair flies apart, subject to the constant confining force given by the string tension σ; this results in hyperbolic motion [21] of the type discussed in the previous section. At $t = 0$, the q and $\bar{q}$ separate with an initial velocity $v_0 = p/\sqrt{p^2 + m^2}$, where $p \simeq \sqrt{s}/2$ is the momentum of the primary constituents in the overall CMS and m the effective quark mass. We now have to solve (31) with this situation as boundary condition; the force

$$F = \sigma\,, \tag{40}$$

is given by the string tension σ binding the $q\bar{q}$ system. The solution is

$$\tilde{x} = \left[1 - \sqrt{1 - v_0\tilde{t} + \tilde{t}^2}\right]\,, \tag{41}$$

with $\tilde{x} = x/x_0$ and $\tilde{t} = t/x_0$; here the scale factor

$$x_0 = \frac{m}{\sigma}\frac{1}{\sqrt{1 - v_0^2}} = \frac{1}{a}\gamma \tag{42}$$

is the inverse of the acceleration a measured in the overall CMS. The velocity becomes

$$v(t) = \frac{{\rm d}x}{{\rm d}t} = \frac{(v_0/2) - \tilde{t}}{\sqrt{1 - v_0\tilde{t} + \tilde{t}^2}}\,; \tag{43}$$

it vanishes for

$$\tilde{t}^* = \frac{v_0}{2} \Rightarrow t^* = \frac{v_0}{2}\frac{m}{\sigma}\gamma\,, \tag{44}$$

thus defining

$$x(t^*) = \frac{m}{\sigma}\gamma\left(1 - \sqrt{1 - (v_0^2/4)}\right) \simeq \frac{\sqrt{s}}{2\sigma} \tag{45}$$

as classical turning point and hence as the classical event horizon measured in the overall CMS (see Fig. 3).

Equation (45) allows the q and the $\bar{q}$ to separate arbitrarily far, provided the pair has enough initial energy; this clearly violates color confinement. Our mistake was to consider the $q\bar{q}$ system as classical; in quantum field theory, it is not possible to increase the potential energy of a given $q\bar{q}$ state beyond the threshold value necessary to bring a virtual $q\bar{q}$ pair on-shell. In QED, the corresponding phenomenon was addressed by Schwinger [53], who showed that in the presence of a constant electric field of strength $\mathcal{E}$ the probability of producing an electron–positron pair is given by

$$P(M, \mathcal{E}) \sim \exp\left\{-\pi m_{\rm e}^2/e\mathcal{E}\right\}\,, \tag{46}$$

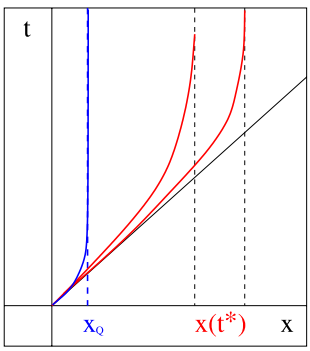

Fig. 3. Classical and quantum horizons in $q\bar{q}$ separation

with m_e denoting the electron mass and e denoting the electric charge. This result is in fact a specific case of the Hawking–Unruh phenomenon, as shown in [23, 24]. In QCD, we expect a similar effect when the string tension exceeds the pair production limit, i.e., when

$$\sigma x > 2m\,, \tag{47}$$

where m specifies the effective quark mass. Beyond this point, any further stretching of the string is expected to produce a $q\bar{q}$ pair with the probability

$$P(M,\sigma) \sim \exp\{-\pi m^2/\sigma\}\,, \tag{48}$$

with the string tension σ replacing the electric field strength $e\mathcal{E}$. This string breaking acts like a quantum event horizon $x_q = 2m/\sigma$, which becomes operative long before the classical turning point is ever reached (see Fig. 3). Moreover, the resulting allowed separation distance for our $q\bar{q}$ pair, the color confinement radius x_Q, does not depend on the initial energy of the primary quarks.

There are some important differences between QCD and QED. In the case of the latter, the initial electric charges, which lead to the field $\mathcal{E}$, can exist independently in the physical vacuum, and the produced pair can be simply ionized into an e^+ and an e^-. In contrast, neither the primary quark nor the constituents of the $q\bar{q}$ pair have an independent existence, so that in string breaking color neutrality must be preserved. As a result, the Hawking radiation in QCD must consist of $q\bar{q}$ pairs, and these can be produced in an infinite number of different excitation states of increasing mass and degeneracy. Moreover, the $q\bar{q}$ pair spectrum is itself determined by the strength σ of the field, in contrast to the exponent $m_e^2/\mathcal{E}$ in (46), where the value of $\mathcal{E}$ has no relation to the electron mass m_e.

Hadron production in e^+e^- annihilation is believed to proceed in the form of a self-similar cascade [54, 55]. Initially, we have the separating primary $q\bar{q}$ pair,

$$\gamma \to [q\bar{q}]\,, \tag{49}$$

where the square brackets indicate color neutrality. When the energy of the resulting color flux tube becomes large enough, a further pair $q_1\bar{q}_1$ is excited from the vacuum by two-gluon exchange (see Fig. 4),

$$\gamma \to [q[\bar{q}_1 q_1]\bar{q}]\,. \tag{50}$$

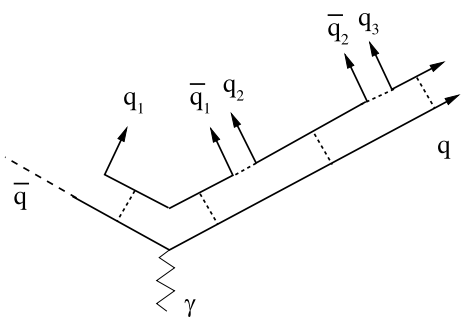

Fig. 4. String breaking through $q\bar{q}$ pair production

Although the new pair is at rest in the overall CMS, each of its constituents has a transverse momentum k_T determined, through the uncertainty relation, by the transverse dimension r_T of the flux tube. The slow $\bar{q}_1$ now screens the fast primary q from its original partner $\bar{q}$, with an analogous effect for the q_1 and the primary antiquark. To estimate the $q\bar{q}$ separation distance at the point of pair production, we recall that the thickness of the flux tube connecting the $q\bar{q}$ pair is in string theory given by [58]

$$r_T = \sqrt{\frac{2}{\pi\sigma}} \sum_{k=0}^{K} \frac{1}{k+1}\,, \tag{51}$$

where K is the string length in units of an intrinsic vibration measure. Lattice studies [60] show that for strings in the range of 1–2 fm, the first string excitation dominates, so that we have

$$r_T = c_0 \sqrt{\frac{2}{\pi\sigma}}\,, \tag{52}$$

with $c_0 \simeq 1$ or slightly larger. Higher excitations lead to a greater thickness and eventually to a divergence (the "roughening" transition). From the uncertainty relation we then have

$$k_T = \frac{1}{c_0}\sqrt{\frac{\pi\sigma}{2}}\,. \tag{53}$$

With this transverse energy included in (47), we obtain for the pair production separation x_Q

$$\begin{aligned} \sigma x_q = 2\sqrt{m^2 + k_T^2} \Rightarrow x_q &\simeq \frac{2}{\sigma}\sqrt{m^2 + (\pi\sigma/2c_0^2)} \\ &\simeq \sqrt{\frac{2\pi}{\sigma c_0^2}} \simeq 1\,\mathrm{fm}\,, \end{aligned} \tag{54}$$

with $\sigma = 0.2\,\mathrm{GeV}^2$, $m^2 \ll \sigma$, and $c_0 \simeq 1$.

Once the new pair is present, we have a color neutral system $q\bar{q}_1 q_1\bar{q}$; but since there is a sequence of connecting string potentials $q\bar{q}_1$, $\bar{q}_1 q_1$ and $q_1\bar{q}$, the primary string is not yet broken. To achieve that, the binding of the new pair has to be overcome, i.e., the q_1 has to tunnel through the barrier of the confining potential provided by $\bar{q}_1$, and vice versa. Now the q exerts a longitudinal force on the $\bar{q}_1$, the $\bar{q}$ on the q_1, resulting in a longitudinal acceleration and ordering of q_1 and $\bar{q}_1$. When (see Fig. 4)

$$\sigma x(q_1\bar{q}_1) = 2\sqrt{m^2 + k_T^2}\,, \tag{55}$$

the $\bar{q}_1$ reaches its $q_1\bar{q}_1$ horizon; on the other hand, when

$$\sigma x(q\bar{q}_1) = 2\sqrt{m^2 + k_T^2}\,, \tag{56}$$

the new flux tube $q\bar{q}_1$ reaches the energy needed to produce a further pair $q_2\bar{q}_2$. The $\bar{q}_2$ screens the primary q from the q_1 and forms a new flux tube $q\bar{q}_2$. At this point, the original string is broken, and the remaining pair $\bar{q}_1 q_2$ form a color neutral bound state which is emitted as Hawking radiation in the form of hadrons, with the relative weights of the

different states governed by the corresponding Unruh temperature. The resulting pattern is schematically illustrated in Fig. 4.

To determine the temperature of the hadronic Hawking radiation, we return to the original pair excitation process. To produce a quark of momentum $k_{\rm T}$, we have to bring it on-shell and change its velocity from zero to $v = k_{\rm T}/(m^2 + k_{\rm T}^2)^{1/2} \simeq 1$. This has to be achieved in the time of the fluctuation determined by the virtuality of the pair, $\Delta\tau = 1/\Delta E \simeq 1/2k_{\rm T}$. The resulting acceleration thus becomes

$$a = \frac{\Delta v}{\Delta\tau} \simeq 2k_{\rm T} \simeq \sqrt{2\pi\sigma}/c_0 \simeq 1\,\text{GeV}\,, \tag{57}$$

which leads to

$$T_{\rm Q} = \frac{a}{2\pi} \simeq \frac{1}{c_0}\sqrt{\frac{\sigma}{2\pi}} \simeq 160\text{–}180\,\text{MeV}\,, \tag{58}$$

for the hadronic Unruh temperature. It governs the momentum distribution and the relative species abundances of the emitted hadrons.

A given step in the evolution of the hadronization cascade of a primary quark or antiquark produced in e^+e^- annihilation thus involves several distinct phenomena. The color field created by the separating q and $\bar{q}$ produces a further pair $q_1\bar{q}_1$ and then provides an acceleration of the q_1, increasing its longitudinal momentum. When it reaches the $q_1\bar{q}_1$ confinement horizon, still another pair $q_2\bar{q}_2$ is excited; the state $\bar{q}_1 q_2$ is emitted as a hadron, the $\bar{q}_2$ forms together with the primary q a new flux tube. This pattern thus step by step increases the longitudinal momentum of the "accompanying" $\bar{q}_i$ as well as of the emitted hadron. This, together with the energy of the produced pairs, causes a corresponding deceleration of the primary quarks q and $\bar{q}$, in order to maintain overall energy conservation. In Fig. 5, we show the world lines given by the acceleration $\bar{q}_i \to \bar{q}_{i+1}$ ($q_i \to q_{i+1}$) and the formation threshold of the hadrons $\bar{q}_i q_{i+1}$ and the corresponding antiparticles.

The energy loss and deceleration of the primary quark q in this self-similar cascade, together with the acceleration of the accompanying partner $\bar{q}_i$ from the successive pairs brings q and $\bar{q}_i$ closer and closer to each other in momentum, from an initial separation $q\bar{q}_1$ of $\sqrt{s}/2$, until they finally are combined into a hadron and the cascade is ended. The resulting pattern is shown in Fig. 6.

The number of emitted hadrons, the multiplicity $\nu(s)$, follows quite naturally from the picture presented here.

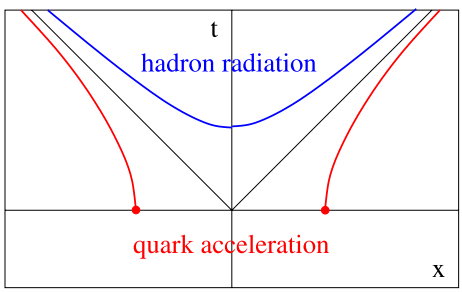

Fig. 5. Quark acceleration and hadronization world lines

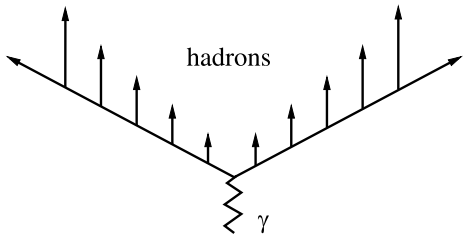

Fig. 6. Hadronization in e^+e^- annihilation

The classical string length, in the absence of quantum pair formation, is given by the classical turning point determined in (45). The thickness of a flux tube of such an "overstretched" string is known [58]; instead of (51) we have

$$R_{\rm T}^2 = \frac{2}{\pi\sigma}\sum_{k=0}^{K}\frac{1}{2k+1} \simeq \frac{2}{\pi\sigma}\ln 2K\,, \tag{59}$$

where K was the string length in units of an intrinsic string vibration measure. From (45) we thus get

$$R_{\rm T}^2 \simeq \frac{2}{\pi\sigma}\ln\sqrt{s} \tag{60}$$

for the flux tube thickness in the case of the classical string length. In parton language, the logarithmic growth of the transverse hadron size is due to a random walk of the parton ("Gribov diffusion" [59]); this phenomenon is responsible for diffraction cone shrinkage in high energy hadron scattering.

Because of pair production, the string breaks whenever it is stretched to the length x_q given in (54); its thickness $r_{\rm T}$ at this point is given by (51). The multiplicity can thus be estimated by the ratio of the corresponding classical to quantum transverse flux tube areas,

$$\nu(s) \sim \frac{R_{\rm T}^2}{r_{\rm T}^2} \sim \ln\sqrt{s}\,, \tag{61}$$

and it is found to grow logarithmically with the e^+e^- annihilation energy, as is observed experimentally over a considerable range.

We note here that in our argumentation we have neglected parton evolution, which would cause the emitted radiation (e.g., $\bar{q}_1 q_2$ in Fig. 4) to start another cascade of the same type. Such evolution effects result eventually in a stronger increase of the multiplicity. The formation of a white hole does not affect the production of hard processes at early times (e.g., multiple jet production), which is responsible for an additional growth of the measured multiplicity.

A further effect we have not taken into account here is parton saturation. At sufficiently high energy, stronger color fields can lead to gluon saturation and thus to a higher temperature determined by the saturation momentum [23, 24]. The resulting system then expands and hadronizes at the universal temperature determined by the string tension.

It interesting to compare the separation of two energetic light quarks, as we have considered here, with that of

two static heavy quarks Q and $\bar{Q}$. From quarkonium studies it is known that

$$2(M_D - m_c) \simeq 2(M_B - m_b) \simeq 1.2\,\mathrm{GeV}\,, \tag{62}$$

where M_D (M_B) and m_c (m_b) are the masses of open charm (beauty) mesons and of the corresponding charm (beauty) quarks, respectively. The energy needed to separate a heavy $Q\bar{Q}$ pair thus is independent of the mass of the heavy quarks, indicating that the string breaking involved here is really a consequence of the vacuum, through $q\bar{q}$ pair excitation. With

$$\sigma x_{\mathrm{Q}} \simeq 1.2\,\mathrm{GeV} \Rightarrow x_{\mathrm{Q}} \simeq 1.2\,\mathrm{fm} \tag{63}$$

we find that the resulting separation threshold for pair excitation agrees well with that found above in (54). Lattice QCD studies lead to similar results.

Up to now, we have considered hadron production in e^+e^- annihilation, in which the virtual photon produces a confined colored $q\bar{q}$ pair as a "white hole". Turning now to hadron–hadron collisions, we note that here two incident white holes combine to form a new system of the same kind, as schematically illustrated in Fig. 7. Again the resulting string or strong color field produces a sequence of $q\bar{q}$ pairs of increasing CMS momentum, leading to the well-known multiperipheral hadroproduction cascade shown in Fig. 8. We recall here the comments made above concerning parton evolution and saturation; in hadronic collisions as well, these phenomena will affect the multiplicity, but not the relative abundances.

In the case of heavy ion collisions, two new elements enter. The resulting systems could now have an overall baryon number, up to $B = 400$ or more. To take that into account, we need to consider the counterpart of charged black holes. Furthermore, in heavy ion collisions the resulting hadron production can be studied as a function of centrality, and peripheral collisions could lead to an interaction region with an effective overall angular momentum. Hence we will also consider rotating black holes. In the next section, we then summarize the relevant features of black holes with $Q \neq 0, J \neq 0$.

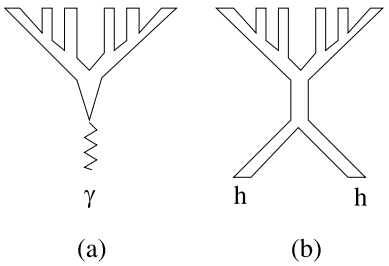

Fig. 7. "White hole" structure in e^+e^- annihilation **a** and hadronic collisions **b**

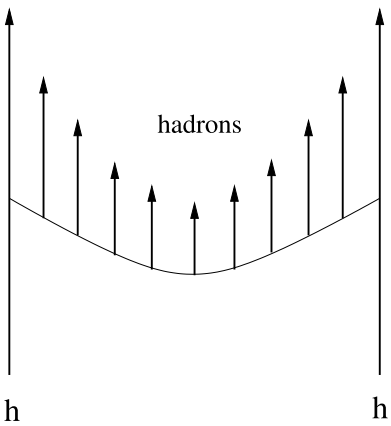

Fig. 8. Hadronization in hadron–hadron collisions

5 Charged and rotating black holes

As mentioned, for an outside observer the only characteristics of a black hole are its mass M, its electric charge Q, and its spin or angular momentum J. Hence any further observables, such as the event horizon or the Hawking temperature, must be expressible in terms of these three quantities.

The event horizon of a black hole is created by the strong gravitational attraction, which leads to a diverging Schwarzschild metric at a certain value of the spatial extension R. Specifically, the invariant space-time length element $\mathrm{d}s^2$ is at the equator given by

$$\mathrm{d}s^2 = (1 - 2GM/R)\,\mathrm{d}t^2 - \frac{1}{1 - 2GM/R}\,\mathrm{d}r^2\,, \tag{64}$$

with r and t for flat space and time coordinates; it is seen to diverge at the Schwarzschild radius $R_{\mathrm{S}} = 2GM$. If the black hole has a net electric charge Q, the resulting Coulomb repulsion will oppose and hence weaken the gravitational attraction; this will in turn modify the event horizon. As a result, the corresponding form (denoted as Reissner–Nordström metric) becomes

$$\mathrm{d}s^2 = (1 - 2GM/R + GQ^2/R^2)\,\mathrm{d}t^2 - \frac{1}{1 - 2GM/R + GQ^2/R^2}\,\mathrm{d}r^2\,. \tag{65}$$

For this case, the divergence leads to the smaller Reissner–Nordström radius

$$R_{\mathrm{RN}} = GM(1 + \sqrt{1 - Q^2/GM^2})\,, \tag{66}$$

which reduces to the Schwarzschild radius R_{S} for $Q = 0$. The temperature of the Hawking radiation now becomes [37, 56]

$$T_{\mathrm{BH}}(M,Q) = T_{\mathrm{BH}}(M,0)\left\{\frac{4\sqrt{1 - Q^2/GM^2}}{(1 + \sqrt{1 - Q^2/GM^2})^2}\right\}\,; \tag{67}$$

its functional form is illustrated in Fig. 9. We note that with increasing charge, the Coulomb repulsion weakens the gravitational field at the event horizon and hence decreases the temperature of the corresponding quantum excitations. As $Q^2 \to GM^2$, the gravitational force is fully compensated and there is no more Hawking radiation.

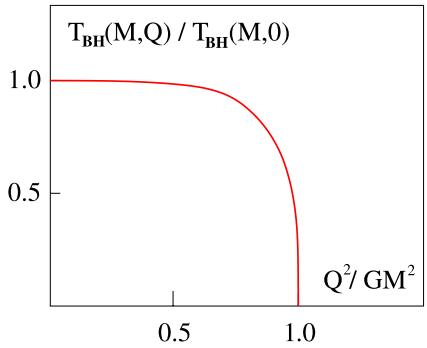

Fig. 9. Radiation temperature for a charged black hole

In a similar way, the effect of the angular momentum of a rotating black hole can be incorporated. It is now the centripetal force that counteracts the gravitational attraction and hence reduces its strength. The resulting Kerr metric must take into account that in this case the rotational symmetry is reduced to an axial symmetry, and, with θ denoting the angle relative to the polar axis $\theta = 0$, it is (at fixed longitude) given by

$$\mathrm{d}s^2 = \left(1 - \frac{2GMR}{R^2 + j^2\cos^2\theta}\right)\mathrm{d}t^2 - \frac{R^2 + j^2\cos^2\theta}{R^2 - 2GMR + j^2}\mathrm{d}r^2 - (R^2 + j^2\cos^2\theta)\,\mathrm{d}\theta^2\,. \tag{68}$$

The angular momentum of the black hole is here specified by the parameter $j = J/M$; for $a = 0$, we again recover the Schwarzschild case. The general situation is now somewhat more complex, since (68) leads to two different divergence points. The solution

$$R_{\mathrm{K}} = GM(1 + \sqrt{1 - j^2/(GM)^2}) \tag{69}$$

defines the actual event horizon, corresponding to absolute confinement. But the resulting black hole is now embedded in a larger ellipsoid,

$$R_{\mathrm{E}} = GM(1 + \sqrt{1 - [j^2/(GM)^2]\cos^2\theta})\,, \tag{70}$$

as illustrated in Fig. 10. The two surfaces touch at the poles, and the region between them is denoted as the ergosphere. Unlike the black hole proper, communication between the ergosphere and the outside world is possible. Any

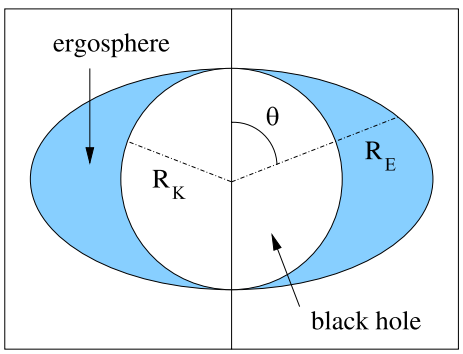

Fig. 10. Geometry of a rotating black hole

object in the ergosphere will, however, suffer from the rotational drag of the rotating black hole and thereby gain momentum. We shall return to this shortly; first, however, we note that the temperature of the Hawking radiation from a rotating black hole becomes

$$T_{\mathrm{BH}}(M, J) = T_{\mathrm{BH}}(M, 0)\left\{\frac{2\sqrt{1 - j^2/(GM)^2}}{1 + \sqrt{1 - j^2/(GM)^2}}\right\}. \tag{71}$$

For a non-rotating black hole, with $j = 0$, this also reduces to the Hawking temperature for the Schwarzschild case.

To illustrate the effect of the ergosphere, imagine radiation from a Schwarzschild black hole emitted radially outward from the event horizon. In the case of a Kerr black hole, such an emission is possible only along the polar axis; for all other values of θ, the momentum of the emitted radiation (even light) will increase due to the rotational drag in the ergosphere. This effect ceases only once the radiation leaves the ergosphere. Since the amount of drag depends on θ, the momentum of the radiation emitted from a rotating black hole, as measured at large distances, will depend on the latitude at which it is emitted and increase from pole to equator.

Finally, for completeness, we note that for black holes with both spin and charge (denoted as Kerr–Newman), the event horizon is given by

$$R_{\mathrm{KN}} = GM(1 + \sqrt{1 - [Q^2/GM^2] - [j^2/(GM)^2]})\,, \tag{72}$$

and the radiation temperature becomes [37, 56]

$$T_{\mathrm{BH}}(M, Q, J) = T_{\mathrm{BH}}(M, 0, 0) \times \left\{\frac{4\sqrt{1 - (GQ^2 + j^2)/(GM)^2}}{(1 + \sqrt{1 - (GQ^2 + j^2)/(GM)^2})^2 + j^2/(GM)^2}\right\}. \tag{73}$$

The decrease of T_{BH} for $Q \neq 0, J \neq 0$ expresses the fact that both the Coulomb repulsion and the rotational force counteract the gravitational attraction, and if they win, the black hole is dissolved.

The dependence of a black hole on its basic properties M, Q and J is very similar to the dependence of a thermodynamic system on a set of thermodynamic observables. The first law of thermodynamics can be written as

$$\mathrm{d}E = T\,\mathrm{d}S + \phi\,\mathrm{d}Q + \omega\,\mathrm{d}J\,, \tag{74}$$

expressing the variation of the energy with entropy S, charge Q and spin J; here ϕ denotes the electrostatic potential per charge and ω the rotational velocity. The corresponding relation in black hole thermodynamics becomes

$$\mathrm{d}M = T_{\mathrm{BH}}\,\mathrm{d}S_{\mathrm{BH}} + \Phi\,\mathrm{d}Q + \Omega\,\mathrm{d}J\,, \tag{75}$$

where the entropy S_{BH} is defined as the area of the event horizon,

$$S_{\mathrm{BH}} = \frac{\pi\left(R_{\mathrm{KN}}^2 + j^2\right)}{G}\,. \tag{76}$$

The temperature is given by (73), and

$$\Phi = \frac{4\pi Q R_{\rm RN}}{G S_{\rm BH}}\,, \quad \Omega = \frac{4\pi a}{S_{\rm BH}} \tag{77}$$

specify the electrostatic potential Φ and the rotational velocity Ω.

The considerations of this section were for spherical black holes. As seen above, such objects are in fact equivalent to uniformly accelerating systems. An application to actual high energy collisions involves a further assumption. Thermal Hawking–Unruh radiation arises already from a single $Q\bar{Q}$ system, as seen above in the discussion of e^+e^- annihilation. If we treat the systems produced in heavy ion collisions as black holes of an overall baryon number and/or an overall spin, we are assuming that the collision leads to a large-scale collective system, in which each accelerating parton is affected by the totality of the other accelerating partons. This assumption clearly goes beyond our event horizon conjecture and, in particular, it need not be correct in order to obtain thermal hadron production.

6 Baryon density and angular momentum

6.1 Vacuum pressure and baryon repulsion

We now want to consider the extension of charged black hole physics to color confinement in the case of collective systems with a net baryon number. In (67) we had seen that the reduction of the gravitational attraction by Coulomb repulsion in a charged black hole modifies the event horizon and hence in turn also the temperature of Hawking radiation. The crucial quantity here is the ratio Q^2/GM^2 of the repulsive overall Coulomb force, Q^2/R^2, to the attractive overall gravitational force, GM^2/R^2, at the horizon.

In QCD, we have a "white" hole containing colored quarks, confined by chromodynamic forces or, equivalently, by the pressure of the physical vacuum. If the system has a non-vanishing overall baryon number, the baryon number dependent interaction will also affect the forces at the event horizon. The simplest instance of such a force is the repulsion between quarks due to Fermi statistics, but more generally, there will be repulsive effects of the type present in cold dense baryonic matter, such as neutron stars. The resulting pressure will modify the confinement horizon and hence lead to a corresponding modification of the Hawking–Unruh temperature of hadronization.

By using the conjectured correspondence between black hole thermodynamics and the thermodynamics of confined color charges, we translate black hole mass, charge and gravitational constant into white hole energy, net baryon number and string tension,

$$\{M, Q, G\} \leftrightarrow \{E, B, 1/2\sigma\}\,. \tag{78}$$

Hence (67) leads us to the relation

$$T_{\rm Q}(B) = T_{\rm Q}(B=0)\left\{\frac{4\sqrt{1-2\sigma B^2/E^2}}{(1+\sqrt{1-2\sigma B^2/E^2})^2}\right\}; \tag{79}$$

for the dependence of the hadronization temperature on the ratio of net baryon number B and energy E, with $T_{\rm Q}(B=0)$ given by (58). Its functional form is the same as that illustrated in Fig. 9.

It would be interesting to test the prediction (79) against the experimental data; one could identify B with the net baryon number per unit rapidity $\mathrm{d}N_{\rm B}/\mathrm{d}y$ and E with the total transverse energy per unit rapidity $\mathrm{d}E_{\rm T}/\mathrm{d}y$. The reduction of the hadronization temperature with baryon number could thus occur in two ways. A sufficient decrease of the collision energy, e.g. from peak SPS to AGS energy, will strongly reduce $\mathrm{d}E_{\rm T}/\mathrm{d}y$, while $\mathrm{d}N_{\rm B}/\mathrm{d}y$ is not affected as much. This leads to the known decrease of $T(\mu_{\rm B})$ with increasing $\mu_{\rm B}$ [61], and it will be interesting to see if the form (79) agrees with the observed behavior. A second, novel possibility would be to consider hadrochemistry as a function of rapidity. At peak SPS energy, $\mathrm{d}N_{\rm B}/\mathrm{d}y$ remains essentially constant up to about $y = 2$, while $\mathrm{d}E_{\rm T}/\mathrm{d}y$ drops by more than a factor of two from $y = 0$ to $y = 2$ [62]. A similar behavior occurs at still lower collision energies. Hence it would seem worthwhile to check if an abundance analysis at large y indeed shows the expected decrease of the hadronization temperature.

6.2 Angular momentum and non-central collisions

The dependence of Hawking radiation on the angular momentum of the emitting system introduces another interesting aspect for the "white hole evaporation" we have been considering. Consider a nucleus–nucleus collision at non-zero impact parameter b. If the interaction is of collective nature, the resulting interaction system may have some angular momentum orthogonal to the reaction plane (see Fig. 11). In central collisions, this will not be the case, nor for extremely peripheral ones, where one expects essentially just individual nucleon–nucleon collisions without any collective effects.

If it possible to consider a kinematic region in which the interacting system does have an overall spin, then the resulting Hawking radiation temperature should be correspondingly reduced, as seen in (71). The effect is not so easily quantified, but simply a reduction of the hadronization temperature for non-central collisions would be quite indicative. Such a reduction could appear only in the temperature determined by the relative abundances, since, as we shall see shortly, the transverse momentum

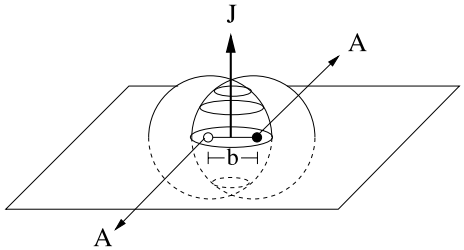

Fig. 11. Rotating interaction region in non-central AA collision

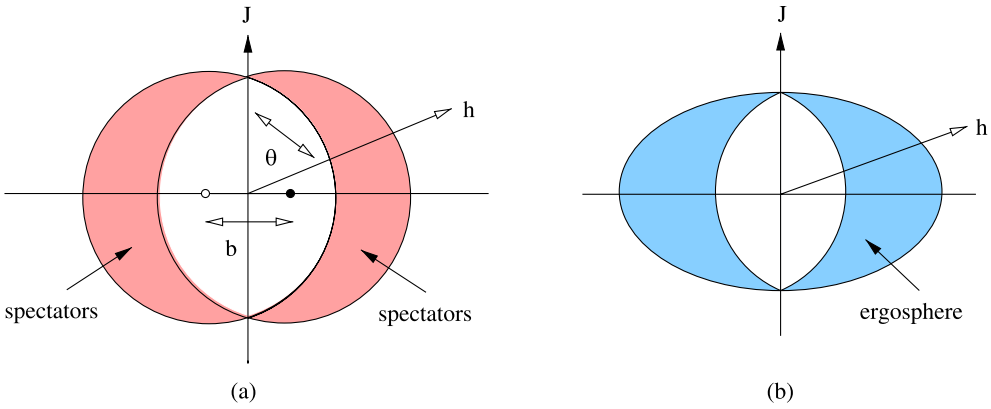

Fig. 12. Transverse plane view of a non-central AA collision

spectra should show modifications due to the role of the ergosphere.

We next turn to the momentum spectrum of the Hawking radiation emitted from a rotating white hole. As discussed in Sect. 4, such radiation will exhibit an azimuthal asymmetry due to the presence of the ergosphere, which by its rotation will affect the momentum spectrum of any passing object. At the event horizon, the momentum of all radiation is determined by the corresponding Hawking temperature (71); but the passage of the ergosphere adds rotational motion to the emerging radiation and hence increases its momentum. As a result, only radiation emitted directly along the polar axis will have momenta as specified by the Hawking temperature; with increasing latitude θ (see Fig. 12a), the rotation will increase the radiation momentum up to a maximum value in the equatorial plane.

Hawking radiation from a rotating source thus leads for nuclear collisions quite naturally to what in hydrodynamic studies is denoted as elliptic flow. It is interesting to note that both scenarios involve collective effects: while in hydrodynamics, it is assumed that non-central collisions lead to an azimuthally anisotropic pressure gradient, we have here assumed that such collisions lead to an overall angular momentum of the emitting system.

Concluding this section we emphasize that the results obtained here for the Hawking temperatures of systems with finite baryon density or with an effective overall spin depend crucially on the assumption of collectivity. If the various nucleon–nucleon interactions in a heavy ion collision do not result in sufficiently collective behavior, the corresponding modifications of T_q do not apply. In the case of black holes with spin, we moreover have no way to relate in a quantitative way centrality and overall spin. Both cases do show, however, that such extensions lead to qualitatively reasonable modifications.

7 Temperature and acceleration limits

We have seen that the underlying confinement dynamics of high energy hadron collisions and e^+e^- annihilation led to a limit on the acceleration (or the corresponding deceleration) in the self-similar hadronization cascade – a limit that can be specified in terms of the string tension. In turn, this led to a limiting Unruh hadronization temperature,

$$T_{\rm Q} \simeq \sqrt{\frac{\sigma}{2\pi}}\,. \tag{80}$$

We emphasize that a Hawking–Unruh temperature as such can a priori have any value; it is the universal limit on the acceleration that leads to a universal temperature for the emitted hadron radiation.

In the study of strongly interacting matter, temperature limits are well known and arise for an ideal gas of different composite constituents ("resonances" or "fireballs" of varying mass M), if the composition law provides a sufficiently fast increase of the degeneracy $\rho(M)$ with M. If the number of states of a constituent of mass M grows exponentially,

$$\rho(M) \sim M^{-a} \exp\{bM\}\,, \tag{81}$$

with constants a and b, then the grand canonical partition function for an ideal gas in a volume V,

$$\mathcal{Z}(T,V) = \sum_N \frac{1}{N!} \times \left[\frac{V}{(2\pi)^3}\int {\rm d}M\rho(M)\int {\rm d}^3p \exp\left\{-\sqrt{p^2+M^2}/T\right\}\right]^N, \tag{82}$$

diverges for

$$T > T_{\rm H} \equiv 1/b\,, \tag{83}$$

so that the Hagedorn temperature $T_{\rm H}$ [26,27] constitutes an upper limit for the temperature of hadronic matter.

In the dual resonance model [63,64], the resonance composition pattern is governed by linearly rising Regge trajectories,

$$\alpha' M_n^2 = n + \alpha_0\,, \quad n = 1, 2, \ldots\,, \tag{84}$$

in terms of the universal Regge slope $\alpha' \simeq 1\,{\rm GeV}^{-2}$ and a constant (of order unity) specifying the family $(\pi, \rho, \ldots)$. For an ideal resonance gas in $D-1$ space and one time dimension, one then obtains [65]

$$a = \frac{1}{2}(D+1)\,, \quad b = 2\pi\sqrt{\frac{D\alpha'}{6}}\,, \tag{85}$$

leading to the temperature limit

$$T_{\rm R} = \frac{1}{2\pi}\sqrt{\frac{6}{\alpha' D}}\,. \tag{86}$$

In string theory, the Regge resonance pattern is replaced by string excitation modes, retaining the same underlying partition structure, with $\alpha' = 1/2\pi\sigma$ relating Regge slope and string tension. Hence we get

$$T_{\rm R} = \sqrt{\frac{6\sigma}{2\pi D}} \tag{87}$$

for the corresponding limiting temperature. For $D = 4$, this coincides with (1) from [23, 24] and agrees within 20% with the Unruh temperature (80) determined by the lowest string excitation alone ($c_0 = 1$ in (58)).

Prior to the dual resonance model, Hagedorn had determined the level density $\rho(M)$ of fireballs composed of fireballs, requiring the same composition pattern at each level [26, 27]. The resulting bootstrap condition leads to [66]

$$a = 3\,, \quad b = r_0\left[\frac{3\pi}{4}(2\ln 2 - 1)\right]^{-1/3} \simeq r_0\,, \tag{88}$$

where r_0 measures the range of the strong interaction. With $r_0 \simeq 1$ fm, we thus get $T_{\rm H} \simeq 0.2$ GeV for the limiting temperature of hadronic matter. If we identify r_0 with the pair production separation x_q obtained in (54), we get

$$T_{\rm H} = \frac{1}{x_q} \simeq \sqrt{\frac{\sigma}{2\pi}} \tag{89}$$

and hence again agreement with the hadronic Unruh temperature (80).

Hadronic matter as an ideal gas of constituents with self-similar composition spectra ("resonances of resonances" or "fireballs of fireballs") thus leads to an upper limit of the temperature, because the level density of such constituents increases exponentially. What does this have to do with the limiting acceleration found in the $q\bar{q}$ cascade of e^+e^- annihilation?

To address this problem, it is useful to recall the underlying reason for the exponential increase of the level density in the dual resonance model and the bootstrap model. The common origin in both cases is a classical partition problem, which in its simplest form [57] asks: how many ways $\rho(M)$ are there to partition a given integer M into ordered combinations of integers? As example, we have for $M = 4$ the partitions $4, 3+1, 1+3, 2+2, 2+1+1, 1+2+1, 1+1+2, 1+1+1+1$; thus here $\rho(M=4) = 8 = 2^{M-1}$. It can be shown that this is generally valid, so that

$$\rho(M) = \frac{1}{2}\exp\{M\ln 2\}\,. \tag{90}$$

For a "gas of integers", $T_0 = 1/\ln 2$ would thus become the limiting temperature; the crucial feature in thermodynamics is the exponential increase in the level density due to the equal a priori weights given to all possible partitions.

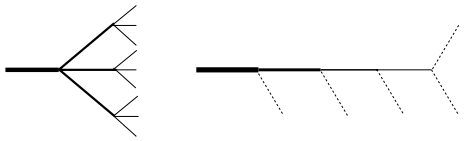

(a) (b)

Fig. 13. Fireball decay patterns

Returning now to the quark cascade in e^+e^- annihilation, we note that the form we have discussed above is a particular limiting case. We assumed that the color field of the separating $q\bar{q}$ excites in the first step one new pair from the vacuum; in principle, though with much smaller probability, it can also excite two or more. The same is true at the next step, when the tunneling produces one further pair: here also, there can be two or more. Thus the e^+e^- cascade indeed provides a partition problem of the same kind. What remains to be shown are the two specific features of our case: that the dominant decay chain is one where in each step one hadron is produced, which provides the constant deceleration of the primary quark and antiquark.

The statistical bootstrap model as well as the dual resonance model leads to self-similar decay cascades, starting from a massive fireball (or resonance), which decays into further fireballs, and so on, until at the end one has light hadrons. In Fig. 13a we illustrate such a cascade for the case where the average number $\bar{k}$ of constituents per step in the decay (or composition) partition pattern

$$\begin{aligned} &M \to M_{11} + M_{12} + \ldots + M_{1k}\,; \\ &M_{11} \to M_{21} + M_{22} + \ldots + M_{2k}\,; \quad \ldots \end{aligned} \tag{91}$$

is $k = 3$. In the statistical bootstrap model, $\bar{k}$ can be can be determined [67]; it is found that the crucial feature here is the power term multiplying the exponential increase in (81). For $a < 5/2$, the distribution in k is given by

$$F(k) = \frac{(\ln 2)^{k-1}}{(k-1)!}\,, \tag{92}$$

so that the average becomes

$$\bar{k} = 1 + 2\ln 2 \simeq 2.4\,. \tag{93}$$

The dominant decay ($\sim 70\%$) is thus into two constituents, with 24% three-body and 6% four-body decays. While in general the fireball mass M could decrease in each step by M/k, i.e., by an amount depending on M, the case $a < 5/2$ is found to be dominated by one heavy and one soft light hadron,

$$M \to M_1 + h_1\,; \quad M_1 \to M_2 + h_2\,; \quad \ldots \tag{94}$$

where h_i denotes final hadrons; the pattern is shown in Fig. 13b. Moreover, the three- and four-body decays also lead to one heavy state plus soft light hadrons. The decay thus provides a uniform decrease of the fireball mass by the average hadron mass or transverse energy.

We therefore conclude that the hadronization pattern we have obtained for e^+e^- annihilation is indeed also con-

nected to the same partition problem as the one leading to exponential level densities.

8 Stochastic versus kinetic thermalization

In statistical mechanics, a basic topic is the evolution of a system of many degrees of freedom from non-equilibrium to equilibrium. Starting from a non-equilibrium initial state of low entropy, the system is assumed to evolve as a function of time through collisions to a time-independent equilibrium state of maximum entropy. In other words, the system loses the information about its initial state through a sequence of collisions and thus becomes thermalized. In this sense, thermalization in heavy ion collisions was studied as the transition from an initial state of two colliding beams of "parallel" partons to a final state in which these partons have locally isotropic distributions. This "kinetic" thermalization requires a sufficient density of constituents, sufficiently large interaction cross sections, and a certain amount of time.

From such a point of view, the observation of thermal hadron production in high energy collisions, in particular in e^+e^- and pp interactions, is a puzzle: how could these systems ever "have reached" thermalization? Already Hagedorn [68] had therefore concluded that the emitted hadrons were "born in equilibrium". Given an exponentially increasing resonance mass spectrum, it remained unclear why collisions should result in a thermal system.

Hawking radiation provides a stochastic rather than kinetic approach to equilibrium, with a randomization essentially provided by the quantum physics of the Einstein–Podolsky–Rosen effect. The barrier to information transfer due to the event horizon requires that the resulting radiation states excited from the vacuum are distributed according to maximum entropy, with a temperature determined by the strength of the "confining" field. The ensemble of all produced hadrons, averaged over all events, then leads to the same equilibrium distribution as obtained in hadronic matter by kinetic equilibration. In the case of a very high energy collision with a high average multiplicity already one event can provide such equilibrium; because of the interruption of information transfer at each of the successive quantum color horizons, there is no phase relation between two successive production steps in a given event. The destruction of memory, which in kinetic equilibration is achieved through sufficiently many successive collisions, is here automatically provided by the tunneling process.

So the thermal hadronic final state in high energy collisions is not reached through a kinetic process; it is rather provided by successively throwing dice.

9 Conclusions

We have shown that quantum tunneling through the color confinement horizon leads to thermal hadron production in the form of Hawking–Unruh radiation. In particular, this implies the following.

- The radiation temperature $T_{\rm Q}$ is determined by the transverse extension of the color flux tube, giving

$$T_{\rm Q} \simeq \sqrt{\frac{\sigma}{2\pi}}\,, \tag{95}$$

  in terms of the string tension σ.
- The multiplicity $\nu(s)$ of the produced hadrons is approximately given by the increase of the flux tube thickness with string length, leading to

$$\nu(s) \simeq \ln\sqrt{s}\,, \tag{96}$$

  where $\sqrt{s}$ denotes the CMS collision energy. Parton evolution and gluon saturation will, however, increase this, as will early hard production. The universality of the resulting abundances is, however, not affected.
- The temperature of Hawking radiation can in general depend on the charge and the angular momentum of the emitting system. The former here provides a baryon number dependence of the hadronization temperature and predicts a decrease of $T_{\rm Q}$ for sufficiently high baryon density. The latter provides the basis for the possibility of elliptic flow and of a dependence of $T_{\rm Q}$ on the centrality of AA collisions.
- The limiting temperature obtained in the statistical bootstrap and the dual resonance or string model arises from a self-similar composition pattern leading to an exponentially growing level density. We find that the underlying partition problem also leads to the cascade form obtained for hadron emission in high energy collisions, so that the dynamic and the thermodynamic limits have the same origin.
- In statistical QCD, thermal equilibrium is reached kinetically from an initial non-equilibrium state, with memory destruction through successive interactions of the constituents. In high energy collisions, tunneling prohibits information transfer and hence leads to stochastic production, so that we have a thermal distribution from the outset.

We close with a general comment. In astrophysics, Hawking–Unruh radiation has so far never been observed. The thermal hadron spectra in high energy collisions may thus indeed be the first experimental instance of such radiation, though in strong interaction instead of gravitation.

Acknowledgements. D.K. is grateful to E. Levin and K. Tuchin for useful and stimulating discussions. H.S. thanks M. Kozlov for helpful discussions and a critical reading of the text. The work of D.K. was supported by the U.S. Department of Energy under Contract No. DE-AC02-98CH10886.

References

1. E. Recami, P. Castorina, Lett. Nuovo Cimento **15**, 347 (1976)
2. A. Salam, J. Strathdee, Phys. Rev. D **18**, 4596 (1978)
3. C.J. Isham, A. Salam, J. Strathdee, Phys. Rev. D **3**, 867 (1971)

4. D.J. Gross, F. Wilczek, Phys. Rev. Lett. **30**, 1343 (1973)
5. H.D. Politzer, Phys. Rev. Lett. **30**, 1346 (1973)
6. J.R. Ellis, Nucl. Phys. B **22**, 478 (1970)
7. R.J. Crewther, Phys. Lett. B **33**, 305 (1970)
8. M.S. Chanowitz, J.R. Ellis, Phys. Lett. B **40**, 397 (1972)
9. J. Schechter, Phys. Rev. D **21**, 3393 (1980)
10. J.C. Collins, A. Duncan, S.D. Joglekar, Phys. Rev. D **16**, 438 (1977)
11. N.K. Nielsen, Nucl. Phys. B **120**, 212 (1977)
12. A.A. Migdal, M.A. Shifman, Phys. Lett. B **114**, 445 (1982)
13. D. Kharzeev, E. Levin, K. Tuchin, Phys. Lett. B **547**, 21 (2002)
14. D. Kharzeev, E. Levin, K. Tuchin, Phys. Rev. D **70**, 054 005 (2004)
15. M.A. Shifman, A.I. Vainshtein, V.I. Zakharov, Nucl. Phys. B **147**, 385 (1979)
16. J.M. Maldacena, Adv. Theor. Math. Phys. **2**, 231 (1998) [Int. J. Theor. Phys. **38**, 1113 (1999)]
17. S.W. Hawking, Commun. Math. Phys. **43**, 199 (1975)
18. W.G. Unruh, Phys. Rev. D **14**, 870 (1976)
19. A.F. Grillo, Y. Srivastava, Phys. Lett. B **85**, 377 (1979)
20. S. Barshay, W. Troost, Phys. Lett. B **73**, 437 (1978)
21. A. Hosoya, Prog. Theor. Phys. **61**, 280 (1979)
22. M. Horibe, Prog. Theor. Phys. **61**, 661 (1979)
23. D. Kharzeev, K. Tuchin, Nucl. Phys. A **753**, 316 (2005)
24. D. Kharzeev, Nucl. Phys. A **774**, 315 (2006)
25. D. Kharzeev, E. Levin, K. Tuchin, Phys. Rev. C **75**, 044 903 (2007) [arXiv:hep-ph/0602063]
26. R. Hagedorn, Nuovo Cim. Suppl. **3**, 147 (1965)
27. R. Hagedorn, Nuovo Cim. A **56**, 1027 (1968)
28. F. Becattini, Z. Phys. C **69**, 485 (1996)
29. F. Becattini, U. Heinz, Z. Phys. C **76**, 268 (1997)
30. J. Cleymans, H. Satz, Z. Phys. C **57**, 135 (1993)
31. F. Becattini et al., Phys. Rev. C **64**, 024 901 (2001)
32. P. Braun-Munziger, K. Redlich, J. Stachel, in: Quark-Gluon Plasma 3, eds. by R.C. Hwa, X.N. Wang (World Scientific, Singapore, 2003), p. 491
33. M. Cheng et al., Phys. Rev. D **74**, 054 507 (2006)
34. T.D. Lee, Nucl. Phys. B **264**, 437 (1986)
35. M.K. Parikh, F. Wilczek, Phys. Rev. Lett. **85**, 5042 (2000)
36. J. Dias de Deus, C. Pajares, hep-ph/0605148
37. Li Zhi Fang, R. Ruffini, Basic Concepts in: Relativistic Astrophysics (World Scientific, Singapore, 1983)
38. J.D. Bekenstein, Phys. Rev. D **7**, 2333 (1973)
39. R. Alkofer, C.S. Fischer, F.J. Llanes-Estrada, Phys. Lett. B **6111**, 279 (2005)
40. M. Novello et al., Phys. Rev. D **61**, 045 001 (2000)
41. T.D. Lee, in: Statistical Mechanics of Quarks and Hadrons, ed. by H. Satz (North Holland Publishing Co., Amsterdam, 1980)
42. H. Pagels, E.T. Tomboulis, Nucl. Phys. B **143**, 453 (1978)
43. P. Castorina, M. Consoli, Phys. Rev. D **35**, 3249 (1987)
44. L.B. Abbott, Nucl. Phys. B **185**, 189 (1981)
45. L. Maiani et al., Nucl. Phys. B **273**, 275 (1986)
46. D. Kharzeev, J. Raufeisen, nucl-th/0206073
47. U.H. Gerlach, Int. J. Mod. Phys. A **11**, 3667 (1996)
48. H. Terashima, Phys. Rev. D **61**, 104 016 (2000)
49. A. Einstein, B. Podolsky, N. Rosen, Phys. Rev. **47**, 777 (1935)
50. Y. Aharanov, D. Bohm, Phys. Rev. **108**, 1070 (1957)
51. W. Pauli, Relativitätstheorie, in: Enzyklopädie der mathematischen Wissenschaften (Teubner, Leipzig, 1921) [English version: Theory of Relativity (Pergamon Press, London, 1958)]
52. R. Laflamme, Phys. Lett. B **196**, 449 (1987)
53. J. Schwinger, Phys. Rev. **82**, 664 (1951)
54. J.D. Bjorken, Lect. Notes Phys. (Springer) **56**, 93 (1976)
55. A. Casher, H. Neuberger, S. Nussinov, Phys. Rev. D **20**, 179 (1979)
56. S. Iso, H. Umetsu, F. Wilczek, hep-th/0606018
57. P. Blanchard, S. Fortunato, H. Satz, Eur. Phys. J. C **34**, 361 (2004)
58. M. Lüscher, G. Münster, P. Weisz, Nucl. Phys. B **180**, 1 (1981)
59. V.N. Gribov, arXiv:hep-ph/0006158
60. G. Bali, K. Schilling, C. Schlichter, Phys. Rev. D **51**, 5165 (1995)
61. F. Becattini et al., Phys. Rev. C **64**, 024 901 (2001)
62. NA49 Collaboration, F. Sikler et al., Nucl. Phys. A **661**, 45 (1999)c
63. S. Fubini, G. Veneziano, Nuovo Cim. **64A**, 811 (1969)
64. K. Bardakci, S. Mandelstam, Phys. Rev. **184**, 1640 (1969)
65. K. Huang, S. Weinberg, Phys. Rev. Lett. **25**, 895 (1970)
66. W. Nahm, Nucl. Phys. B **45**, 525 (1972)
67. S. Frautschi, Phys. Rev. D **3**, 2821 (1971)
68. R. Hagedorn, Thermodynamics of Strong Interactions, CERN 71-12, 1971